Resistivity Model for Soft Magnetic Composite Materials with Cauer Network Representation

Joonas Vesa[1,2], Hajime Igarashi[2], Antero Marjamäki[1], Reda Elkhadrawy[1], and Paavo Rasilo[1]
[1]Electrical Engineering Unit, Tampere University, Tampere 33014, Finland
[2]Graduate School of Information Science and Technology, Hokkaido University, Sapporo 061-0814, Japan

A Cauer network -like resistivity model is proposed for soft magnetic composite materials. The model is immediately available in both time- and frequency domains. The network components are expressed as closed form analytical expressions. The component values and thus the resistivity depend explicitly on the physical and geometric properties of the material, and no empirical fitting parameters are introduced. Using the resistivity model together with a similar kind of reluctivity model, we find that a macroscale magnetodynamic finite element model of a toroid is consistent with measurements. The proposed methods provide a numerically efficient and an easy-to-use framework to model soft magnetic composites.

I. Introduction

Soft magnetic composites (SMC) consist of electrically insulated ferromagnetic powder. The powder is compressed into the shape of a component and heat-treated [1]. Fig. 1 depicts a microscope image showing some of the particles.

Modeling such materials with particle-like structures requires special techniques, since the particle scale phenomena affect the behavior of the whole material. A very important example of such a phenomenon are the local eddy currents inside the particles. It has been proposed in the literature to lump these local eddy currents into a complex permeability [2] or its time domain extensions [3]. Such models are neat, since they allow to model the composite as a single homogeneous continuum material.

However, it has been addressed in the literature, that some SMC materials have nonzero macroscale conductivity [4]. In this case, it is still possible to lump the intra-particle eddy currents into a dynamic magnetic model, but another model for resistivity is needed to account for the inter-particle eddy currents. In this article, a resistivity model is proposed for SMC materials in the form of a Cauer-like network. The model takes into account the powder-like structure of such materials and it depends explicitly on the mean particle diameter, the particle diameter variance, and the insulation thicknesses of the material. Explicit dependencies on other physical features, such as particle permeability, particle conductivity, insulation permittivity, and insulation conductivity, are also present. No empirical fitting parameters that have no clear physical meaning are introduced. The aim is to keep the material models as simple as possible while having both time- and frequency domains immediately available.

II. Methods

We introduce the resistivity model as a part of a larger numerical example. The novelty of this paper is contained in Section II-B, but we must also discuss the reluctivity model, the finite element (FE) formulation, and the measurements.

Manuscript received June 14th, 2024; revised Aug. 6th, 2024. Corresponding author: J. Vesa (https://researchportal.tuni.fi/fi/persons/joonas-vesa).

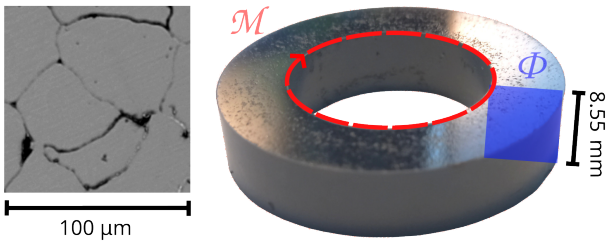

Fig. 1. Microscope image (left). Toroid sample (right).

A. Reluctivity

Previously [5], [6], a complex-valued reluctivity was derived for SMC materials in the form

$$\begin{cases} \nu_l(\omega) & = \frac{1}{(1+\tau)\eta}\left[\frac{\tau}{\mu_{\text{ins}}} + \frac{1}{\mu}\frac{RkJ_0(Rk)}{2J_1(Rk)}\right], \\ \nu_{\text{num}}(\omega) & = \frac{\int_L lg(l)\nu_l(\omega)\mathrm{d}l}{\int_L lg(l)\mathrm{d}l}, \end{cases} \tag{1}$$

where τ is the relative insulation thickness, η is the volume fraction, μ_{ins} is the insulation permeability, μ is the particle permeability, R is the particle radius, J_0 and J_1 are the Bessel functions of the zeroth and first order, and $k^2 = -\mu\sigma j\omega$, where σ is the particle conductivity, j is the imaginary unit, ω is the angular frequency and g is a particle count density function. A summary of the symbols is in Table I. In (1), a model ν_{num} for the homogeneous material is obtained by a numerical integration of single-particle models ν_l over the distribution. It was proposed in [6] to approximate the model (1) as a single-particle model

$$\nu(\omega) = \frac{1}{(1+\tau)\eta}\left[\frac{\tau}{\mu_{\text{ins}}} + \frac{1}{\mu}\frac{R_{\text{eff}}kJ_0(R_{\text{eff}}k)}{2J_1(R_{\text{eff}}k)}\right] \tag{2}$$

that contains an effective particle radius R_{eff}. Assuming that the particle volumes are beta-distributed, R_{eff} can be solved analytically. Equating (1) and (2) in the low- and high frequency limits, we get

$$R_{\text{eff}} = \frac{1}{2}\frac{(l_{\max}-\mu_G)\mu_G^2 - (2l_{\max}+\mu_G)\sigma_G^2}{(l_{\max}-\mu_G)\mu_G - 3\sigma_G^2}, \tag{3}$$

where $l_{\max}$ is the maximal particle diameter, and μ_{G} and σ_{G}^2 are the expectance and the variance of the particle diameters

in a beta-distributed particle volume density. The technical manipulations that lead to R_{eff} are left for [6]. Furthermore, the recurrence formula (11) was used to expand (2) into a continued fraction, which has the Cauer network representation shown in Fig. 2. The explicit forms of the components

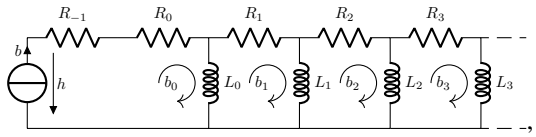

Fig. 2. Cauer network representation of (2).

$$R_{-1} = \frac{\tau}{\mu_{\text{ins}}(1+\tau)\eta}, \tag{4}$$

$$R_i = \frac{1+2i}{\mu(1+\tau)\eta}, \tag{5}$$

$$L_i = \frac{\sigma R_{\text{eff}}^2}{8(i+1)(1+\tau)\eta}, \tag{6}$$

were extracted from the continued fraction expansion. In this paper, we simply use the model (3)-(6) for the reluctivity.

B. Resistivity

In the big picture, we would like to do the same treatment for resistivity what was done for reluctivity. We would like to have a resistivity model, which lumps the inter-particle conductive- and displacement currents into one effective model. This would allow to model the composite as a single homogeneous continuum. In a parallel study [7], a resistivity model ρ_{num} for ferrites was proposed. It is complex-valued and of the form

$$\begin{cases} \rho_l(\omega) & = \frac{1}{(1+\tau)\eta}\left[\frac{\tau}{\sigma_{\text{ins}}+j\omega\varepsilon_{\text{ins}}} + \frac{1}{\sigma}\frac{RkJ_0(Rk)}{2J_1(Rk)}\right], \\ \rho_{\text{num}}(\omega) & = \frac{\int_L lg(l)\rho_l(\omega)\mathrm{d}l}{\int_L lg(l)\mathrm{d}l}, \end{cases} \tag{7}$$

where σ_{ins} is the insulation conductivity, related to inter-particle currents, ε_{ins} is the insulation permittivity, related to inter-particle displacement currents, and all the other parameters are as discussed in Section II-A and summarized in Table I. In (7), the resistivity of the homogeneous material ρ_{num} is obtained by numerically integrating single-particle models ρ_l. What is left to do, is to simplify the model (7) into a Cauer-like network with every component having a closed form expression consisting of only the physical parameters of the material. That is the main contribution of this paper.

Let us approximate the model (7), as in [7], by

$$\rho(\omega) = \frac{1}{(1+\tau)\eta}\left[\frac{\tau}{\sigma_{\text{ins}}+j\omega\varepsilon_{\text{ins}}} + \frac{1}{\sigma}\frac{R_{\text{eff}}kJ_0(R_{\text{eff}}k)}{2J_1(R_{\text{eff}}k)}\right], \tag{8}$$

where the physical parameters are as in (7), but in addition, there is an effective particle radius R_{eff}, which is a result of an "averaging process" of the SMC powder. This "averaging process" is done by equating the models (7) and (8) at the low- and high frequency limits. Specifically, we solve R_{eff} from

$$\lim_{\omega\to 0^+}\rho_{\text{num}}(\omega) = \lim_{\omega\to 0^+}\rho(\omega), \tag{9}$$

$$\lim_{\omega\to\infty}\frac{1}{k}\rho_{\text{num}}(\omega) = \lim_{\omega\to\infty}\frac{1}{k}\rho(\omega). \tag{10}$$

It turns out that (9) holds for any R_{eff}. Given that the associated particle volume density is beta-distributed, it follows from (10) that R_{eff} must be exactly as stated in (3). Since the concrete manipulations are rather long and technical, a reader who wishes to repeat the manipulations is directed to the previous study related to the reluctivity side [6].

Let us now turn our model (8) into a continued fraction expansion. A recurrence formula for Bessel functions [8]

$$2\nu J_\nu(z) = zJ_{\nu-1}(z) + zJ_{\nu+1}(z) \tag{11}$$

can be used to turn (8) into

$$\rho(\omega) = \frac{\tau}{(\sigma_{\text{ins}}+j\omega\varepsilon_{\text{ins}})(1+\tau)\eta} + \frac{1}{\sigma(1+\tau)\eta} + \cfrac{1}{\cfrac{(8\cdot 1)(1+\tau)\eta}{\mu R_{\text{eff}}^2 j\omega} + \cfrac{1}{\cfrac{3}{\sigma(1+\tau)\eta} + \cfrac{1}{\cfrac{(8\cdot 2)(1+\tau)\eta}{\mu R_{\text{eff}}^2 j\omega} + \cfrac{1}{\cfrac{5}{\sigma(1+\tau)\eta} + \cdots}}}}. \tag{12}$$

The model (12) has an interpretation as a circuit. Fig. 3 depicts this circuit, and the component values are given as

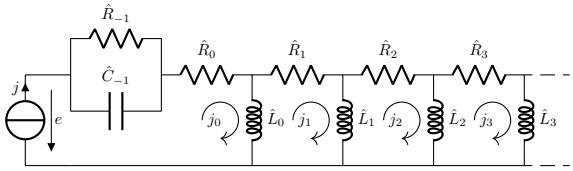

Fig. 3. Cauer-like network representation of (8).

$$\hat{R}_{-1} = \frac{\tau}{\sigma_{\text{ins}}(1+\tau)\eta}, \tag{13}$$

$$\hat{C}_{-1} = \frac{\varepsilon_{\text{ins}}(1+\tau)\eta}{\tau}, \tag{14}$$

$$\hat{R}_i = \frac{1+2i}{\sigma(1+\tau)\eta}, \tag{15}$$

$$\hat{L}_i = \frac{\mu R_{\text{eff}}^2}{8(i+1)(1+\tau)\eta}. \tag{16}$$

The contribution of this article is condensed in (13)-(16).

C. Finite Element Model

Now that the homogenized material models have been defined, let us model the dynamics of the whole toroid we see in Fig. 1. Due to cylindrical symmetry, it suffices to model only one 2-D cross-section of the toroid. Such a cross-section has been indicated by the blue surface in Fig. 1. The proposed models ν and ρ can be used in a magnetodynamic problem

$$\nabla\times\rho(\omega)\nabla\times\mathbf{H} = -j\omega\nu^{-1}(\omega)\mathbf{H}, \tag{17}$$

where the magnetic field strength $\mathbf{H}$ is pointing perpendicularly to the 2-D modeling domain. Furthermore, we set a boundary condition for the cartesian out-of-plane component of $\mathbf{H}$ as

$$H_{\text{z}}(r) = \frac{\mathcal{M}}{2\pi r}, \tag{18}$$

where r is the radial coordinate and $\mathcal{M}$ is the magnetomotive force over the red loop depicted in Fig. 1. By adjusting this

TABLE I
MATERIAL PARAMETERS

Parameter	Explanation	Value
R_{out}	Toroid outer diameter	19.9 mm
R_{in}	Toroid inner diameter	12.1 mm
h_{core}	Toroid thickness	8.6 mm
μ_{G}	Expected particle diameter	101 µm
σ_{G}	Particle diameter deviation	43.4 µm
l_{max}	Maximal particle diameter	$10\mu_{\text{G}}$
μ_{ins}	Insulation permeability	μ_0
η	Volume fraction	0.90
μ	Particle permeability	$871\mu_0$
σ	Particle conductivity	$1.99{\cdot}10^6$ S/m
σ_{ins}	Insulation conductivity	0.235 S/m
ε_{ins}	Insulation permittivity	$136\varepsilon_0$
τ	Insulation thickness (relative)	0.219 %

boundary condition, we can impose the magnetomotive force. Magnetic flux Φ is then computed from the numerical solutions by integrating the flux density over the cross-sectional surface. The relation of the magnetomotive force and the flux is then scaled to have the unit of a complex-valued relative permeability. We set

$$\mu_{\text{homog}} = \frac{l_{\text{eff}}}{A}\frac{\Phi}{\mathcal{M}}, \tag{19}$$

where A is the area of the cross-section of the toroid, and the effective magnetic path length is

$$l_{\text{eff}} = 2\pi\frac{R_{\text{out}} - R_{\text{in}}}{\ln(R_{\text{out}}/R_{\text{in}})}, \tag{20}$$

where R_{out} and R_{in} are the outer radius and the inner radius of the toroid. The toroid's dimensions are summarized in Table I. We emphasize that (19) does not have a local meaning, since the device-scale eddy currents are lumped into μ_{homog}. It is simply a complex magnetic permeance of the toroid, which is scaled into the units of permeability.

D. Measurements

The ratio of the flux Φ and the magnetomotive force $\mathcal{M}$ was measured using an LCR meter and a commercial fixture. The fixture forms a loop of conductor around the hole of the toroid. The fixture is cylindrically symmetric around the toroid sample to minimize leakage fluxes. Furthermore, a reference measurement without the toroid was performed to compensate the fixture's impedance. The measured ratio of Φ and $\mathcal{M}$ was scaled to have the unit of a permeability according to (19). This measured μ_{meas} is depicted in Fig. 4. For more details about the measurement technique, we refer to the detailed thesis of Dr. Kacki [9] and the market leader Keysight's application note [10].

E. Material Parameters

Let us summarize how each material parameter was acquired for the numerical example. Table I lists each of them. The statistical parameters μ_{G} and σ_{G} were esimated from a microscope image, which is similar but substantially larger than what is depicted in Fig. 1. The maximal particle diameter l_{max} was simply assumed to be an order of magnitude larger than the expected diameter, since it is not possible to exactly

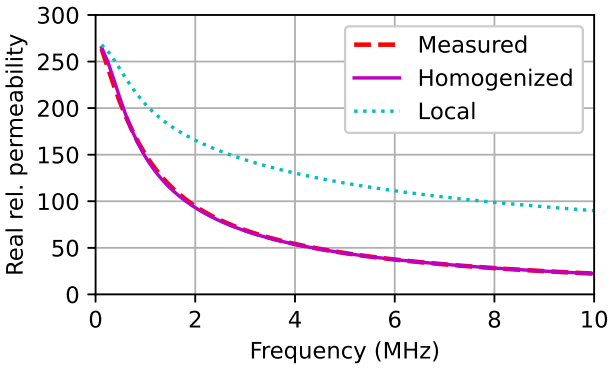

(a)

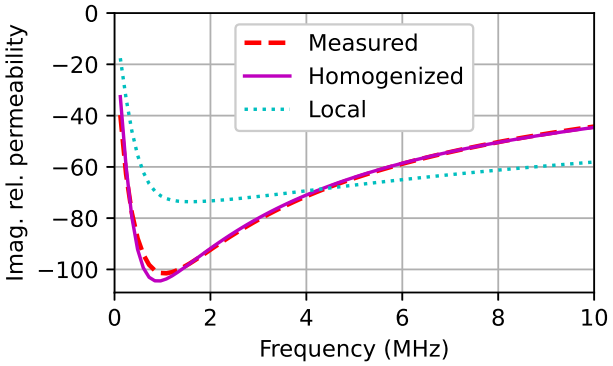

(b)

Fig. 4. Measured and simulated relative permeabilities. (a) Real part. (b) Imaginary part.

know all the particle diameters. The insulation permeability and volume fraction were chosen consistently with the existing literature [5]. It is not possible to measure the parameters μ, σ, σ_{ins}, τ, and ε_{ins}. In the literature, such parameters are searched by inverse estimation techniques [5], [11]. Let us use the least squares -type objective function

$$f(\mu,\sigma,\sigma_{\text{ins}},\tau,\varepsilon_{\text{ins}}) = \sum_f \Big[\text{Re}\Big\{\mu^{-1}_{\text{homog}}(f) - \mu^{-1}_{\text{meas}}(f)\Big\}^2 + \text{Im}\Big\{\mu^{-1}_{\text{homog}}(f) - \mu^{-1}_{\text{meas}}(f)\Big\}^2\Big], \tag{21}$$

which measures a distance between the measured and computed macroscale quantities by evaluating μ_{homog} numerically. The material parameters μ, σ, σ_{ins}, τ, and ε_{ins} are found by minimizing (21) using the reflective trust region minimization algorithm. The estimated parameters are listed in Table I. The values of the estimated parameters seem reasonable. The orders of magnitudes of μ and σ remind of those of metallic materials. The insulation conductivity is low, and the insulations are relatively thin.

III. RESULTS OF THE NUMERICAL EXAMPLE

Fig. 4 illustrates a comparison of the computed "Homogenized" relative permeability with measurements. From the graphs, it is concluded that the model (4)-(6), (13)-(16),

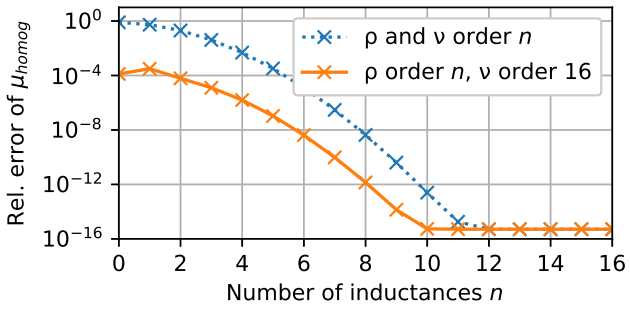

Fig. 5. Convergence of μ_{homog} at 10 MHz.

(17) is consistent with measurements. Furthermore, a "Local" permeability, computed directly from the reluctivity (2) by the formula $1/(\nu_{\text{eff}}\mu_0)$, where μ_0 is the permeability of free space, is also visible in Fig. 4. The discrepancy between the "Local" permeability and the "Homogenized" permeability is important, since it reveals that the macroscale eddy currents are affecting the behavior of the modeled toroid.

What is left to be discussed, is convergence. Let us compute μ_{homog} at 10 MHz using various numbers of inductors for the material models ρ and ν. As an "exact" solution, let us use a computed μ_{homog} in which (2) and (8) serve as material models instead of the Cauer networks. Fig. 5 shows that after adding 12 inductors to both ρ and ν, numerical precision is reached. Furthermore, if ν is of sufficiently high order, the required order of ρ can be read from the lower graph of Fig. 5. If 10^{-4} relative error is chosen as a threshold, ρ should contain at least two inductors. Selecting a lower requirement for convergence, even more coarse truncations are possible. Of course, these numbers are valid only for this particular example.

IV. Conclusion

The main contribution of this article is to propose the analytical formulas for the network components (13)-(16). This network defines a resistivity model for SMC materials. The components depend on the physical parameters of the material, such as expected particle diameter, variance of particle diameters, insulation thickness, insulation permeability, insulation conductivity, insulation permittivity, volume fraction, particle permeability, and particle conductivity. Our numerical example was in frequency domain, but due to the network nature of the material models, time domain is immediately available without numerical Laplace transforms.

Together with the previously presented reluctivity model (4)-(6), the models provide a simple and numerically efficient framework for SMC modeling, which was shown to yield consistent numerical results with measurements up to 10 MHz in our numerical example.

On the other hand, the numerical example showed an interesting result regarding the estimated permeability of the particles. In some of the earlier studies where only the reluctivity side was considered and no device-scale eddy currents were present, the estimated relative particle permeability was some 300 [5], [11]. Such a result was obtained due to the particle permeability being closely linked to the bending of the homogenized permeability curve. Since the toroid's magnetic behavior was assumed to be exactly the same as its local magnetic behavior, this property could not be circumvented. Taking the device-scale eddy currents into account opens up the possibility to have higher relative particle permeability, of the order of some 900. Of course, this quantity cannot be directly measured.

Acknowledgment

This study was mainly funded by the foundation of Ulla Tuominen, a member of the Foundations' Post Doc Pool. This project has received funding from the European Research Council (ERC) under the European Union's Horizon 2020 research and innovation programme (grant agreement No 848590). The Academy of Finland is also acknowledged for financial support (grant No 330062).

References

[1] H. Shokrollahi and K. Janghorban, "Soft magnetic composite materials (SMCs)," *Journal of Materials Processing Technology*, vol. 189, no. 1-3, pp. 1–12, Jul. 2007.

[2] X. Ren, R. Corcolle, and L. Daniel, "A Homogenization Technique to Calculate Eddy Current Losses in Soft Magnetic Composites Using a Complex Magnetic Permeability," *IEEE Transactions on Magnetics*, vol. 52, no. 12, pp. 1–9, Dec. 2016.

[3] Y. Sato and H. Igarashi, "Time-Domain Analysis of Soft Magnetic Composite Using Equivalent Circuit Obtained via Homogenization," *IEEE Transactions on Magnetics*, vol. 53, no. 6, pp. 1–4, Jun. 2017.

[4] A. Bordianu, O. de la Barriere, O. Bottauscio, M. Chiampi, and A. Manzin, "A Multiscale Approach to Predict Classical Losses in Soft Magnetic Composites," *IEEE Transactions on Magnetics*, vol. 48, no. 4, pp. 1537–1540, Apr. 2012.

[5] J. Vesa, L. Hyvärinen, and P. Rasilo, "Eddy-Current Loss Model for Soft Magnetic Composite Materials Considering Particle Size Distribution," *IEEE Transactions on Magnetics*, vol. 59, no. 7, pp. 1–8, Jul. 2023.

[6] J. Vesa, *Complex Reluctivity and Dynamic Hysteresis Model for Soft Magnetic Composite Materials*, arXiv:2408.11597, 2024.

[7] R. Elkhadrawy, V. Tsakaloudi, J. Vesa, and P. Rasilo, "Macroscopic Modeling of Mn-Zn Ferrites Based on Analytical Dynamic Material Models," in *2024 IEEE 21st CEFC*, Jun. 2024, pp. 1–2.

[8] M. Abramowitz and I. A. Stegun, *Handbook of Mathematical Functions With Formulas, Graphs, and Mathematical Tables*, Report, Publisher: United States. Government Printing Office., Dec. 1972.

[9] M. Kacki, "Investigation of the high-frequency effects in Mn-Zn ferrites for EMI filter applications," Ph.D. dissertation, Aug. 2022.

[10] Keysight, *Solutions for Measuring Permittivity and Permeability with LCR Meters and Impedance Analyzers*, Appliction note.

[11] J. Vesa and P. Rasilo, "Permeability and resistivity estimations of SMC material particles from eddy current simulations," *Journal of Magnetism and Magnetic Materials*, vol. 524, p. 167 663, Apr. 2021.